# The environment of FS Tau observed with HST WFPC2 in narrow-band emission line filters

Jens Woitas, Jochen Eislöffel

*Thüringer Landessternwarte Tautenburg, Sternwarte 5, D-07778 Tautenburg, Germany*

woitas@tls-tautenburg.de

jochen@tls-tautenburg.de

Reinhard Mundt

*Max-Planck-Institut für Astronomie, Königstuhl 17, D-69117 Heidelberg, Germany*

mundt@mpia-hd.mpg.de

and

Thomas P. Ray

*School of Cosmic Physics, Dublin Institute for Advanced Studies,
5 Merrion Square, Dublin 2, Ireland*

tr@cp.dias.ie

## ABSTRACT

We present the results of HST WFPC2 observations of FS Tau and its environment obtained in the narrow-band emission line filters H$\alpha$ and [S II] $\lambda\lambda\,6716, 6731$ Å. Based on these data the morphology of line emission within this region can be studied on a size scale of $0\overset{''}{.}1$ for the first time.

Despite the fact that FS Tau A has strong forbidden emission lines, there is no evidence for extended emission at these wavelengths beyond $0\overset{''}{.}5$ from the components of this close T Tauri binary system. In the FS Tau B outflow interesting morphological properties can be studied at high spatial resolution. In this jet we find a fine structure where circular or elliptical jet knots are correlated with mimima of the jet width. The overall width of this jet decreases with distance from the source. The FS Tau B jet is thus a rare example of a jet which may

be recollimated far away from its source. The jet is much more prominent in H$\alpha$ than in [S II], while the counterjet shows the opposite behaviour. The line ratio H$\alpha$/[S II] increases with lateral distance from the jet axis, which is indicative of entrainment of ambient material.

*Subject headings:* Interstellar medium: jets and outflows – Stars: individual: FS Tau

## 1. Introduction

The T Tauri star FS Tau A (other designations HBC 383, Haro 6-5 A) is located in the Taurus-Auriga star forming region (SFR) at a distance of $\approx 140\,\text{pc}$ (e. g. Wichmann et al. 1998). The object and its environment show a variety of phenomena typical for SFRs. FS Tau A is a close binary with a projected separation of $\approx 0\overset{\prime\prime}{.}25$ (Simon et al. 1992). The young stellar object FS Tau B (other designations HBC 381, Haro 6-5 B) is located $\approx 20''$ west of FS Tau A. It is associated with a Herbig-Haro jet discovered by Mundt et al. (1984). This jet (HH 157) has a projected length of $\approx 6'$ and a position angle of 56° (Eislöffel & Mundt 1998, hereafter EM98). Since the radial velocities are only $\approx 60\,\text{km\,s}^{-1}$, the jet is probably orientated quite close to the plane of the sky (Mundt, Brugel, & Bührke 1987). There is also a redshifted counterjet that is much less prominent. FS Tau A and B are surrounded by a complex structure of reflection nebulosities.

Krist et al. (1998, hereafter K98) have used the Wide Field Planetary Camera (WFPC2) of the Hubble Space Telescope (HST) to obtain images of the FS Tau field in the broad-band filters F675W (WFPC2 R band) and F814W (WFPC2 I band). Based on these data they have examined the spatial structure of the reflection nebulosities around FS Tau A and B. In this paper we present data obtained with WFPC2 in the narrow-band emission line filters H$\alpha$ and [S II] $\lambda\lambda\,6716, 6731\,\text{Å}$. We will focus on properties of the FS Tau B outflow that has been observed for the first time with a spatial resolution of $\approx 0\overset{\prime\prime}{.}1$ in these emission lines. Details of observations and data reduction will be given in Sect. 2. The results will be presented in Sect. 3 and discussed in Sect. 4.

## 2. Observations and Data Reduction

FS Tau and its surroundings were observed with HST WFPC2 on 1997 August 26. In the narrow-band filter F656N (H$\alpha$) one 1400 s and two 1300 s exposures were obtained. An-

other four images with integration times of 1300 s each were taken in the F673N filter that contains the [S II] emission lines at $\lambda\lambda = 6716, 6731$ Å. Exposures in the broad-band filters F569W and F791W ($3 \times 100$ s each) were used for continuum subtraction. FS Tau A, its surrounding reflection nebula and FS Tau B were placed onto the PC chip that provides the best spatial resolution (pixel scale $0\overset{''}{.}046$/pixel).

The basic data reduction used the standard HST data pipeline described by Holtzman et al. (1995a, 1995b), which was re-run with updated calibration files. The `crrej` task in STSDAS has been used to remove cosmic rays by combining all images taken in the same filter. After correcting for the bad pixels marked in the data quality file a large number of hot or dark pixels remained. Therefore, additional (automatic and manual) bad pixel corrections have been applied. Finally, the images taken with the PC and the three WF chips were mosaiced into one frame. For this purpose the PC images were re-scaled to fit the pixel scale of the three WF chips ($0\overset{''}{.}1$ pixel). The resultant images in H$\alpha$ and [S II] are shown in Fig. 1.

## 3.  Results

### 3.1.  FS Tau A

One goal of our work was to study the spatial structure of line emission close to the components of the FS Tau A binary. It was already mentioned by Cohen & Kuhi (1979) that this system shows equivalent widths EW(H$\alpha$) = 57.3 Å and EW([O I]) = 21.8 Å. Hirth, Mundt, & Solf (1997) have also detected strong emission in [O II], [N II] and [S II] associated with this binary system. White & Ghez (2001) have resolved the FS Tau A binary in H$\alpha$ and found that both components show equivalent widths EW(H$\alpha$) $> 10$ Å which classifies them as classical T Tauri stars that are supposed to show signs of active disk accretion and bipolar outflows according to standard models of young stars and their environment (e. g. Hartmann 1998).

For a further investigation of this line emission we have used the images taken in the broad-band filters F569W and F791W for continuum subtraction. This subtraction is not straightforward because there are strong colour gradients in the reflection nebulae. As the probable best solution we scaled the continuum images in such a way that the large reflection nebula (labeled with R1 in Fig. 1) northeast of FS Tau B disappears after subtraction. This removes the nebulosity around FS Tau A down to a projected distance of $\approx 0\overset{''}{.}5$ from the

binary components. Neither outside nor inside this radius do we find any structure indicative of bipolar lobes or small-scale jets.

## 3.2. The outflow of FS Tau B

In this section we will discuss morphological properties of the FS Tau B jet. Compared to previous studies of this outflow based on images taken from the ground (e.g. Mundt, Ray, & Raga 1991, hereafter MRR91, EM98) the spatial resolution is increased by an order of magnitude using HST. Using the *Tiny Tim* software (Krist 1995) we have calculated model PSFs at the locations of the jet on the WFPC2 chips for the filters used. They have FWHMs of $\approx 0.1''$, which is comparable to the adopted pixel scale. Therefore, the images have not been deconvolved with any PSF. Since the jet is neither visible in the F569W filter, nor in the F791W, no continuum subtraction has been applied for this analysis either.

In the upper panels of Figs. 2 and 3 contour plots of the outflow region in H$\alpha$ and [S II] are given. The jet source (labeled as FS Tau B in Fig. 1) is not visible at optical wavelengths. Following EM98, we assume the source position to be located $0.''8$ southwest of the nearby bright emission knot. This knot is a strong continuum source, but remains visible in H$\alpha$ and [S II] also after the continuum subtraction described in Sect. 3.1. K98 came to the conclusion that this object, and the emission knot next to it in the southwestern direction, are the upper and lower surfaces of an edge-on seen disk around FS Tau B that is centrally illuminated and seen in scattered light from the star. In our continuum images only the bright northeastern knot can be seen that has the same shape as on the images presented by K98. Concerning our data, the southwestern knot is only visible in H$\alpha$ and [S II]. In the K98 data this object is prominent only in the F675W filter that contains the [O I], H$\alpha$, [N II] and [S II] lines. On the other hand, in the F814W filter that only contains weak emission lines like [Fe II] $\lambda\lambda 7688, 8617$ Å it is not significantly above the background level despite the fact that the integration time was more than twice as large as for our F791W observation (700 s compared to 300 s). This has been checked by downloading the WFPC2 data used by K98 from the archive. So this object is probably rather a jet knot than part of a circumstellar disk.

The pear-shaped object close to FS Tau B in the northeastern direction is a reflection nebula (called R1 by EM98) and is therefore not included in the analysis of the jet. In the northeastern direction the jet is invisible over a distance from the source of $d \approx 20''$ in H$\alpha$ and $d \approx 35''$ in [S II]. In H$\alpha$ it reappears showing a structure resembling a bowshock. The intensity maximum of this structure (called knot B by MRR91 and EM98) is at a distance

of $d = 22\overset{''}{.}7$ from the source. According to EM98 this maximum appeared at $d = 18\overset{''}{.}8$ in November 1990. This shift of $3\overset{''}{.}9$ within 6.75 years is roughly in line with the proper motion of $0\overset{''}{.}504\,\mathrm{yr}^{-1}$ derived by EM98 for this jet knot. Following the jet in its downstream direction we can resolve the structure called A by MRR91 and EM98 (see also Fig. 1) into six intensity maxima or jet knots that have a circular or elliptical shape. Note that a large portion of the more distant part of the outflow is not inside the field of view of WFPC2: There are additional jet knots up to a distance of $\approx 6'$ from the source (e.g. EM98).

In [S II], the northeastern part of the jet is much less prominent than in H$\alpha$. Here, the [S II] flux is roughly an order of magnitude smaller than the flux in H$\alpha$. The counterjet shows a completely different behaviour. It is brighter in [S II] than in H$\alpha$, and there is even an additional emission knot to the southwest visible in [S II] which is not seen in H$\alpha$.

To perform a quantitative analysis of the outflow morphology we used a method similar to the one presented by Raga, Mundt, & Ray (1991). We have fitted Gaussian curves to the intensity distribution perpendicular to the jet. In the jet direction the images were usually binned over four pixels. From the Gaussians we obtained the position of the jet centre, the jet width and the intensity at the jet centre. The latter is converted from ADUs to flux using the conversion factors provided by STScI. The same fits were subsequently done for single image columns (without binning). From averaging over the results we have estimated errors for the jet width and the position of the jet centre.

The results are shown in Figs. 2 and 3 (the three lower panels). Between $d = 20''$ and $d = 33''$ a significant shift of the jet centre in the direction perpendicular to the flow axis can be seen in H$\alpha$. The position angle changes by $\approx 10°$ over this range. Another slight change in the outflow direction at $d \approx 35''$ can be seen in both filters (Figs. 2 and 3, second panel). Between $d = 26''$ and $d = 40''$ variations of the jet width as function of distance to the source can be seen. They form a pattern where minima of the jet width correspond to jet knots or flux maxima. If only the maxima or minima of this fine structure are considered, the overall jet width decreases in this region. The same behaviour can also be seen in [S II] although it is not significant with respect to the error bars here. In that filter the jet width is about a factor two smaller than in H$\alpha$.

## 4. Discussion

We have found that the jet width decreases with distance from the source over a large portion of the visible flow as has already been reported by MRR91. A comparison with other morphological studies of Herbig-Haro jets shows that this behaviour is rather unusual: MRR91 have examined nine outflows and found that the jet width usually increases with distance from the source. The only exceptions from this general behaviour were HH 24 G and FS Tau B in which the jet width decreases. For the FS Tau B jet this behaviour is now confirmed by our much higher spatial resolution HST images. MRR91 put forward an idea to explain the unusual appearance of the FS Tau B outflow: They suggest that after an initial phase of strong expansion the jet gets recollimated.

Recollimation of disk winds by the hoop stresses produced by toroidal magnetic fields has been proposed as a mechanism for focusing YSO jets (e. g. Ouyed & Pudritz 1997). This process happens however at distances of $\approx 10\,\mathrm{AU}$ from the star, whereas for the FS Tau B jet the distance between the source and the first optical jet knot is $\approx 3000\,\mathrm{AU}$. Therefore, in this case the appearance of the outflow is probably the result of an interaction between the jet and its external medium: First, the jet overexpands because it moves into a region of very low pressure. Afterwards, it is recollimated by its ambient medium. This interaction produces shocks that make the jet visible again at a projected distance of $\approx 20''$ from the source. This idea could explain the observed H$\alpha$ bow where the flow becomes visible again.

Numerical simulations of such a process have been given by de Gouveia dal Pino, Birkinshaw, & Benz (1996) and de Gouveia dal Pino & Birkinshaw (1996). They have shown that a morphological structure very similar to that of the FS Tau B jet can appear if the density of the ambient medium increases with distance from the source. On the other hand, their simulations produce only very weak shocks if the jet is moving through a region with decreasing density. This could explain the large gap between the source and the first optically visible part of the jet. If the appearance of the FS Tau B jet is interpreted with respect to the mentioned simulations it will primarily reflect density gradients in the ambient medium that are not spherically symmetric around the source. This idea is in line with our finding that the southwestern counterjet is totally different from the northeastern outflow as well in morphology as in its excitation. It also supports the conclusion of K98 that the FS Tau B jet passes through a "dark nebula" northeast of the source.

Another possible mechanism for recollimating the FS Tau B jet is provided by the recent hydrodynamic (Delamarter, Frank, & Hartmann 2000) and magneto-hydrodynamic

(Gardiner, Frank, & Hartmann 2001) simulations of YSO winds propagating into infalling environments. In such simulations not only does the ambient medium help to recollimate any expanding wind through shock-refocusing but focusing is enhanced through the ram pressure of the surrounding medium.

The intensity peaks, which occur in the jet after its first reappearance (region A in Fig. 1), correspond to minima of the jet width. Ray et al. (1996) have observed the HH 30 jet with HST WFPC2 and found a similar behaviour for that outflow. So this may appear as a common phenomenon if a sufficiently high spatial resolution is used. The mentioned jet knots in the FS Tau B jet have circular or elliptical shape, they do not exhibit the morphology of resolved bows. With respect to the recollimation scenario discussed above they may represent regions where the magnetic hoop stresses are maximum (O'Sullivan & Ray 2000). Another possible explanation is that this fine structure is due to temporal and spatial variations within the jet flow itself. In this case the flow would have a "core" region with bright knots surrounded by another region with lower and roughly constant flux density. Such a situation could be explained by the x-wind model of young stellar objects (Shu et al. 2000 and references therein): This theory predicts that only about one half of the jet flow is within a small angle of some degrees around the polar axis while the rest exits in a wide angle wind. A decision between these scenarios cannot be made solely on the basis of our data. For example the proper motion measurements of these small jet knots are required and this cannot be done by comparison with previous ground-based imaging (e.g. EM98) because these images had a too low spatial resolution to resolve morphological structures on comparable size scales. In addition high spatial resolution mm studies are required to determine the characteristics and the kinematics of the ambient environment surrounding FS Tau B. Such observations will have to await the availability of ALMA.

Finally the jet appears much more collimated in [S II] than in Hα where the jet width is about a factor two larger. This means that the line ratio Hα/[S II] is increasing with lateral distance from the jet centre. A similar situation has been found in HST WFPC2 images of the HH 46/47 jet obtained by Heathcote et al. (1996). In this outflow the body of the jet is primarily seen in [S II] emission while the Hα emission merely denotes wisps and filaments at the border of the jet. The finding that the higher excitation line occurs along the edges of the jet suggests that a large fraction of the observed emission is produced by entrainment of ambient material (Hartigan et al 1993).

## REFERENCES

Cohen, M., Kuhi, L.V. 1979, AJ Supp, 41, 743

de Gouveia dal Pino, E.M., Birkinshaw, M., & Benz, W. 1996, ApJ, 460, 111

de Gouveia dal Pino, E.M., & Birkinshaw, M. 1996, ApJ, 471, 832

Delamarter, G., Frank, A., & Hartmann, L. 2000, ApJ, 530, 923

Gardiner, T., Frank, A., & Hartmann, L. 2001, in preparation

Eislöffel, J., & Mundt, R. 1998, AJ, 115, 1554 (EM98)

Hartigan, P., Morse, J.A., Heathcote, S., & Cecil, G. 1993, ApJ, 414, 121

Hartmann, L., 1998, Accretion Processes in Star Formation (Cambridge, UK: Cambridge University Press)

Heathcote S., Morse, J.A., Hartigan, P., Reipurth, B., Schwartz, R.D., Bally, J., Stone, J.M. 1996, AJ, 112, 1141

Hirth, G.A., Mundt, R., & Solf, J. 1997, A&AS, 126, 437

Holtzman, J.A., et al. 1995, PASP, 107, 156

Holtzman, J.A., Burrows, C.J., Casertano, S., Hester, J., Trauger, J.T., Watson, A.M., & Worthey, G. 1995 PASP, 107, 1065

Krist, J. 1995, in ASP Conf. Proc. 77, Astronomical Data Analysis Software and Systems IV, ed. H.E. Payne, & J.J.E. Hayes, (San Francisco: ASP), 349

Krist, J.E., et al. 1998, ApJ, 501, 841 (K98)

Mundt, R., Bührke, T., Fried, J.W., Neckel, T., Sarcander, M., & Stocke, J. 1984, A&A, 140, 17

Mundt, R., Brugel, E.W., & Bührke, T. 1987, ApJ, 319, 275

Mundt, R., Ray, T.P., & Raga, A.C. 1991, A&A, 252, 740 (MRR91)

Raga, A.C., Mundt, R., & Ray, T.P. 1991, A&A, 252, 733

Ray, T.P., Mundt, R., Dyson, Falle, S.A.E.G, & Raga, A.C. 1996, ApJL, 468, 103

O'Sullivan, S., Ray, T.P. 2000, A&A, 363, 355

Ouyed, R., & Pudritz, R.E. 1997, ApJ, 482, 712

Shu, F.H., Najita, J.R., Shang, H., & Li, Z.Y. 2000, in Protostars and Planets IV, ed. V. Mannings, A.P. Boss, & S.S. Russell, (Tucson: The University of Arizona Press), 789

Simon, M., Chen, W.P., Howell, R.R., Benson, J.A., & Slowik, D. 1992, ApJ, 384, 212

White, R., & Ghez, A. 2001, ApJ, 556, 265

Wichmann, R., & et al. 1998, MNRAS, 301, L39

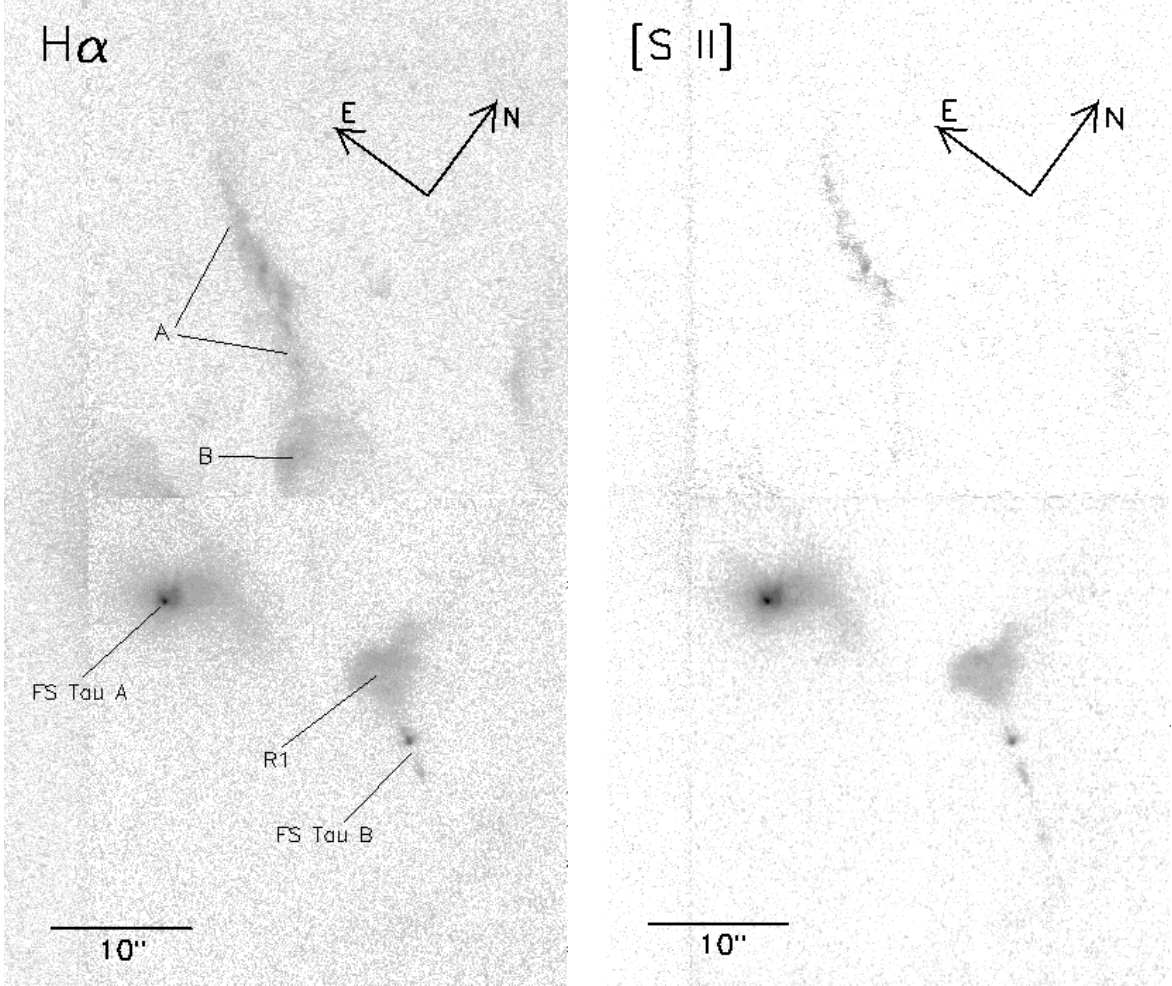Fig. 1.— The FS Tau field in Hα (left panel) and [S II] (right panel) without continuum subtraction. These images are mosaics of parts of the four quadrants of WFPC2, where the images obtained with the PC chip (lower right) have been re-scaled to fit the pixel scale of the three WF chips. The image size is $40 \times 70$ arcsec. The nebulosity around FS Tau A and the structure denoted with R1 are reflection nebulae. The FS Tau B jet is in the upper part of the images, the faint counterjet is located southwest of FS Tau B.
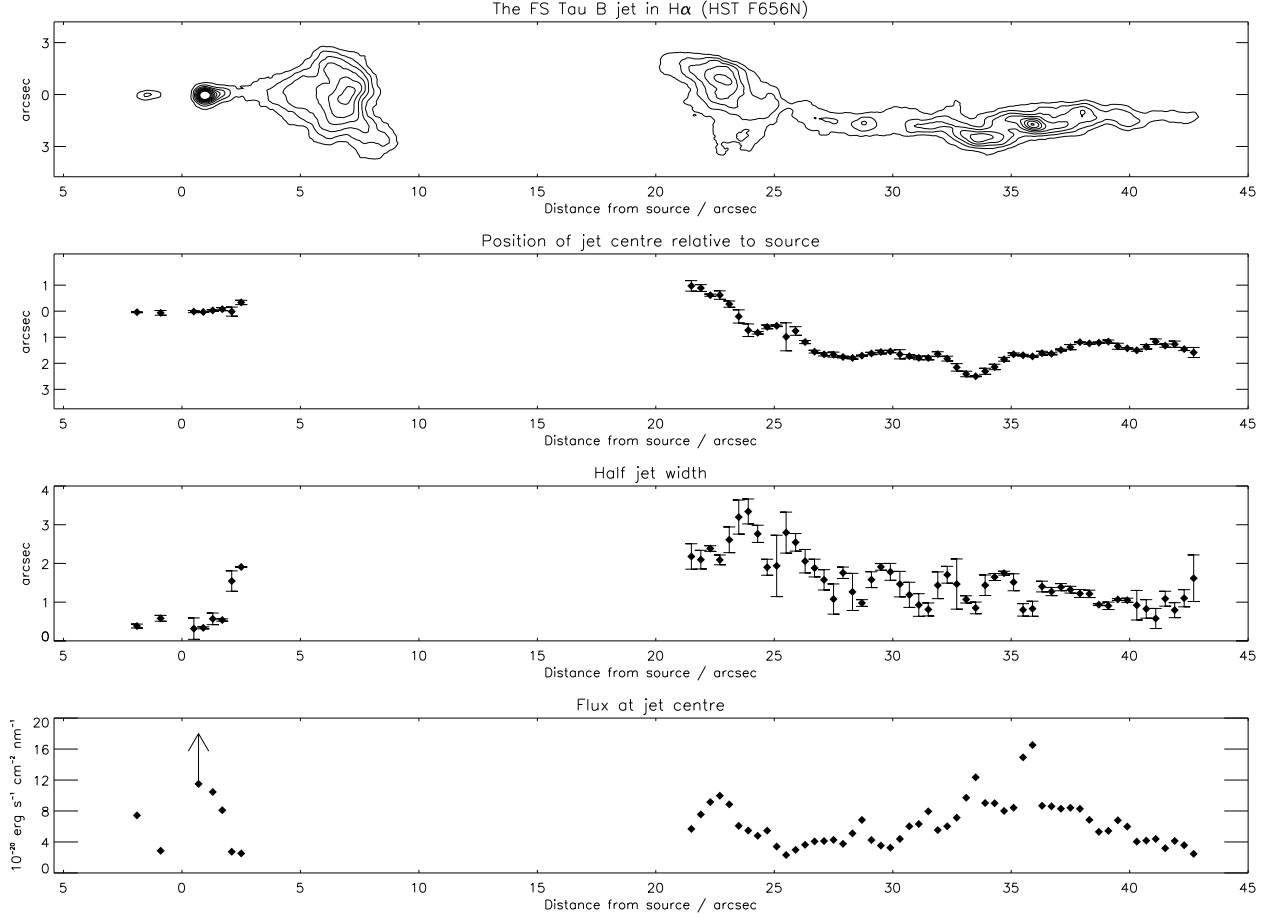
Fig. 2.— The FS Tau B outflow in Hα. The first panel shows a contour plot of the jet (see Fig. 1). The second to fourth panels display the results of the Gaussian fits described in Sect. 3.2: Position of jet centre, half jet width, and intensity at jet centre as function of distance to the source.
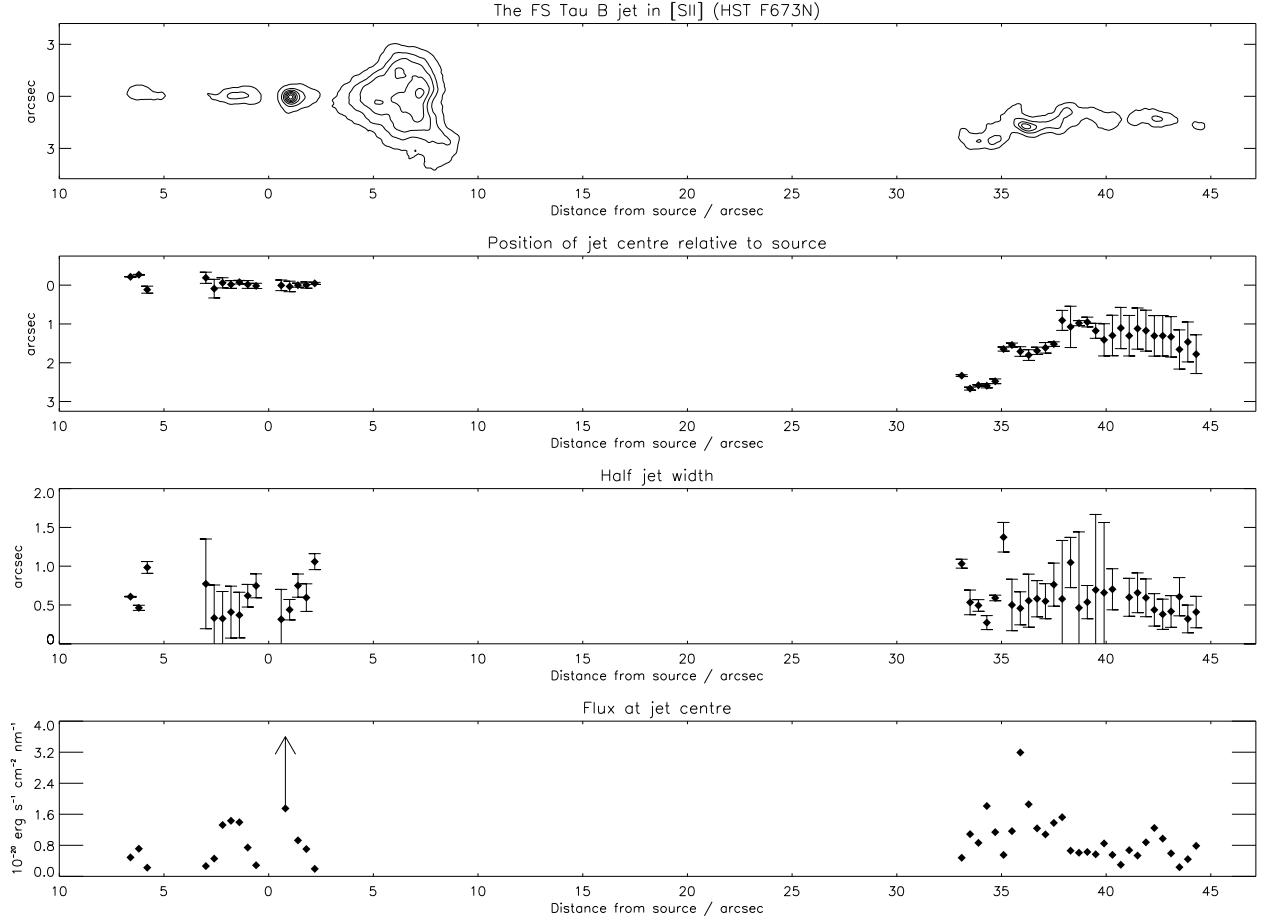
Fig. 3.— The FS Tau B outflow in [S II]. See caption of Fig. 2 for further explanation.